

# Medium- and Long-Distance $^1\text{H}$ – $^{13}\text{C}$ Heteronuclear Correlation NMR in Solids

X. L. Yao, K. Schmidt-Rohr, and M. Hong<sup>1</sup>

Department of Chemistry, Iowa State University, Ames, Iowa 50011

Received September 13, 2000; revised January 2, 2001

**A simple method for obtaining  $^1\text{H}$ – $^{13}\text{C}$  HETCOR solid-state NMR spectra reflecting only medium- and long-range  $^1\text{H}$ – $^{13}\text{C}$  correlation peaks is presented. By dephasing the magnetization of protons directly bonded to a  $^{13}\text{C}$  nucleus, the short-range correlation peaks, which contain limited structural information, can be cleanly suppressed without reducing the long-range cross peaks significantly. The resulting reduction of resonance overlap simplifies spectral assignment. The dephasing of the intensity of a given peak in the HETCOR spectrum traces out a  $^1\text{H}$ – $^{13}\text{C}$  distance-dependent REDOR curve. This medium- and long-distance (MELODI) HETCOR experiment is demonstrated on a mixture of amino acids with  $^{13}\text{C}$  in natural abundance. It is useful for resonance assignment of proteins and other organic solids with partial or no  $^{13}\text{C}$  labeling.**

© 2001 Academic Press

## INTRODUCTION

The correlation of  $^1\text{H}$  and  $^{13}\text{C}$  chemical shifts in solid-state NMR (1, 2) provides useful information on the structure of complex organic materials, including proteins (3), coals (4, 5), soil organic matter (6), and multicomponent polymers (7, 8). However, the information content of peaks correlating directly bonded protons and carbons is often trivial, given the limited  $^1\text{H}$  chemical shift resolution achievable in solids. Aromatic protons are bonded to aromatic carbons, aliphatic protons to aliphatic carbons, peptide  $\alpha$ -protons to  $\alpha$ -carbons, and so on. Structurally more revealing information is obtained from longer-range correlation peaks. These can be excited at longer  $^1\text{H}$ – $^{13}\text{C}$  coherence transfer times, but their identification is usually severely hampered by their overlap with the strong peaks of the directly bonded  $^1\text{H}$ – $^{13}\text{C}$  pairs. In this Communication, we present a simple method for suppressing the one-bond  $^1\text{H}$ – $^{13}\text{C}$  correlation peaks while retaining the medium- and long-range coupling signals. The experiment, termed MELODI-HETCOR for *medium- and long-distance heteronuclear correlation*, employs dephasing of  $^1\text{H}$  magnetization by the nearby  $^{13}\text{C}$  spin, and works for both CH and  $\text{CH}_2$  groups. It is applicable to  $^{13}\text{C}$ -unlabeled materials or to selectively  $^{13}\text{C}$ -labeled systems.

<sup>1</sup> To whom correspondence should be addressed. Fax: (515) 294-0105. E-mail: mhong@iastate.edu.

## PULSE SEQUENCE

Figure 1 displays the pulse sequence of the MELODI-HETCOR experiment. A regular  $^1\text{H}$ – $^{13}\text{C}$  HETCOR experiment, carried out under magic-angle spinning (MAS), is preceded by a constant time of two rotation periods, during which the magnetization of the protons directly bonded to a  $^{13}\text{C}$  nucleus is dephased. The dephasing is driven by  $^{13}\text{C}$ – $^1\text{H}$  dipolar interaction, which is recoupled by a  $^{13}\text{C}$   $180^\circ$  pulse positioned at time  $t_f$  from the beginning of each rotation period. An additional  $^1\text{H}$   $180^\circ$  pulse is applied at the end of the first rotation period to refocus the  $^1\text{H}$  chemical shift interaction and to accumulate the effect of the recoupled  $^{13}\text{C}$ – $^1\text{H}$  dipolar interaction for two rotation periods. To suppress the  $^1\text{H}$ – $^1\text{H}$  homonuclear dipolar interaction, a frequency-switched Lee–Goldburg (FSLG) sequence (9, 10) is applied throughout the two rotation periods. The initial  $^1\text{H}$  magnetization is prepared to be perpendicular to the effective field of the  $^1\text{H}$ – $^{13}\text{C}$  dipolar Hamiltonian by a  $35^\circ$  excitation pulse with the appropriate phase. After the dipolar dephasing period,  $^1\text{H}$  magnetization evolves under the chemical shift interaction during  $t_1$  under homonuclear decoupling. As usual in CRAMPS and HETCOR NMR, the  $^1\text{H}$  carrier frequency was placed off resonance to take advantage of “second averaging” of pulse imperfections (11). This also permits one to restrict the phase cycling to the cosine-modulated component in the indirect dimension of the MELODI-HETCOR spectra. Off-resonance detection has the additional advantage that the zero frequency position, which is often plagued with artifacts in the unfiltered  $^1\text{H}$ – $^{13}\text{C}$  HETCOR spectra, is located at one end of the  $\omega_1$  dimension, away from the resonances of interest.

The FSLG sequence is particularly suited for homonuclear decoupling under high spinning speeds. At slower spinning speeds, other decoupling sequences, such as BLEW-12 (7, 12) or MREV-8 (13), could also be used.

At the end of the  $t_1$  period, the cosine-modulated  $^1\text{H}$  magnetization is flipped back to the  $z$  axis by another  $35^\circ$  pulse of opposite phase. Subsequently, the magnetization is transferred to  $^{13}\text{C}$  spins by either Hartmann–Hahn cross polarization (14) or Lee–Goldburg cross-polarization (3) (LG-CP). Note that standard Hartmann–Hahn CP can be used in the MELODI experiment, even though it does not suppress  $^1\text{H}$  spin diffusion. Spin diffusion

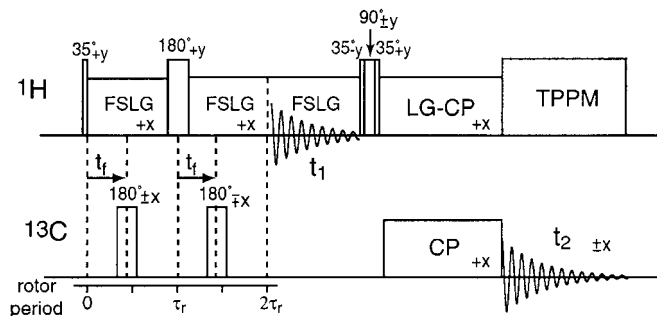


**FIG. 1.** Pulse sequence for the MELODI-HETCOR experiment. The  $^1\text{H}$  chemical shift evolution is preceded by two rotation periods, during which the recoupled  $^{13}\text{C}$ - $^1\text{H}$  dipolar coupling dephases the  $^1\text{H}$  magnetization. The extent of the dipolar dephasing depends on the position of the  $180^\circ$   $^{13}\text{C}$  pulses, which are centered at times  $t_f$  and  $t_f + t_r$ .

does not reintroduce the one-bond correlation peaks suppressed by the MELODI filter. For instance, consider the case in which  $\text{H}\alpha$  has been suppressed through dephasing by  $\text{C}\alpha$ . Thus, there is no evolution at the  $\text{H}\alpha$  frequency. Subsequent transfer from  $\text{H}\beta$  to  $\text{H}\alpha$  to  $\text{C}\alpha$  during Hartmann-Hahn CP will not introduce any  $\omega_1$  signal at the  $\text{H}\alpha$  frequency. However, spin diffusion will lead to an enhancement of long-range peaks relative to medium-distance correlation peaks. If two- and three-bond correlations are specifically of interest, for example, for assignment based on chemical bonding, the more local Lee-Goldburg CP should be employed. This more controlled CP method was used here.

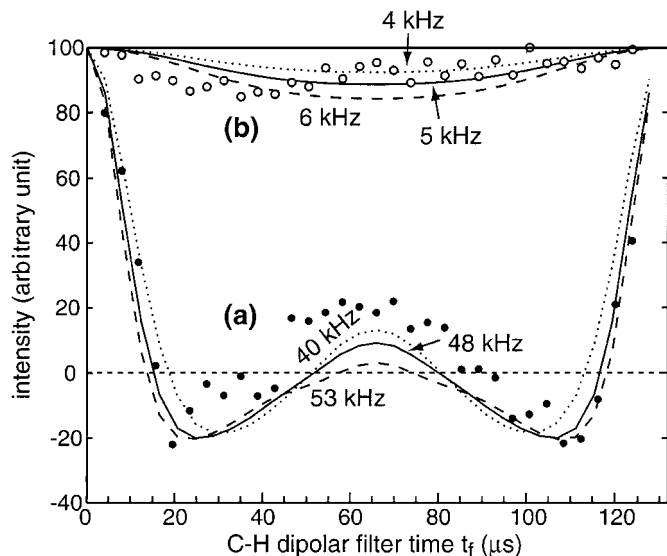


**FIG. 2.** Dipolar dephasing of  $^1\text{H}$  magnetization by  $^{13}\text{C}$  spins as a function of the filter time  $t_f$ . The data were obtained with the sequence of Fig. 1 for  $t_1 = 0$  on  $^{13}\text{C}$ -unlabeled alanine- $d_6$ . (a) Intensity of the  $\text{C}\alpha$  signal (filled circles) represents the  $^1\text{H}$  dephasing behavior of isolated one-bond  $^{13}\text{C}$ - $^1\text{H}$  pairs. (b) Intensity of the  $\text{COO}$  signal (open circles) represents  $^1\text{H}$  dephasing in isolated two-bond  $^{13}\text{CO}$ - $^1\text{H}$  spin pairs. Simulated C-H dephasing curves are shown, with the solid lines indicating the best fits.

It is important to realize that the dephasing of the  $^1\text{H}$  magnetization by nearby  $^{13}\text{C}$  spins applies even to unlabeled systems, where the abundance of  $^{13}\text{C}$  is only 1.1% so that most protons have no  $^{13}\text{C}$  spin nearby. This is because every proton that is detected as a  $^1\text{H}$ - $^{13}\text{C}$  cross peak in a HETCOR spectrum is close to a  $^{13}\text{C}$  spin; from the other protons, no  $^{13}\text{C}$  signals are generated.

## RESULTS AND DISCUSSION

**$^{13}\text{C}$ - $^1\text{H}$  filter time dependence.** Based on the standard C-H bond lengths and bond angles in organic solids, the two-bond  $^{13}\text{C}$ - $^1\text{H}$  dipolar coupling is about seven times weaker than the one-bond  $^{13}\text{C}$ - $^1\text{H}$  interaction. This makes it possible to suppress the magnetization of the one-bond  $^{13}\text{C}$ -coupled protons while retaining that of the more distant protons.

In principle, the dependence of the  $^{13}\text{C}$ - $^1\text{H}$  dephasing on the filter time period  $t_f$  can be determined by recording the intensity of a C-H correlation peak as a function of  $t_f$  in a series of 2D MELODI-HETCOR spectra. However, it is possible to determine this dephasing behavior much more efficiently from a series of 1D  $^{13}\text{C}$  spectra, obtained by applying the MELODI-HETCOR pulse sequence without the  $^1\text{H}$  chemical shift evolution period to a molecule with an isolated proton. We chose alanine- $d_6$  for this purpose. Alanine- $d_6$  contains only one proton ( $\text{H}\alpha$ ) per molecule. Thus, in molecules containing a naturally occurring  $^{13}\text{C}\alpha$  spin, one-bond  $^{13}\text{C}\alpha$ - $^1\text{H}\alpha$  dephasing of the  $\text{H}\alpha$  magnetization can be observed by recording the  $^{13}\text{C}\alpha$  signal as a function of  $t_f$  in a series of 1D spectra. The dephasing of the  $\text{H}\alpha$  magnetization by the naturally abundant  $^{13}\text{COO}$  group two bonds away can be determined from the  $^{13}\text{COO}$  peak intensity in the same spectra. Figure 2 shows the experimental one-bond ( $^{13}\text{C}\alpha$ - $^1\text{H}\alpha$ ) and two-bond ( $^{13}\text{CO}$ - $^1\text{H}\alpha$ ) proton dephasing data as a function of  $t_f$ . As expected, a dramatic difference between the one-bond and the two-bond intensities is observed.

The curves traced out by the data can be regarded as constant-time  $^{13}\text{C}$ - $^1\text{H}$  REDOR (rotational-echo double resonance) curves (15). The C-H dipolar interaction is effectively quadrupled, since the phase acquired by the proton coherence under the action of the recoupled  $^{13}\text{C}$ - $^1\text{H}$  dipolar coupling is  $4 \cdot \Phi(t_f)$  by the end of the two rotation periods (16). Since the homonuclear decoupling sequence reduces the  $^{13}\text{C}$ - $^1\text{H}$  dipolar coupling by a scaling factor  $\kappa_{\text{FSLG}}$ , the effective C-H dipolar coupling is given by

$$\delta_{\text{eff,CH}} = 4 \kappa_{\text{FSLG}} \delta_{\text{CH}}, \quad [1]$$

where  $\delta_{\text{CH}}$  is the unscaled dipolar coupling constant, which is 22.7 kHz for a  $^{13}\text{C}$ - $^1\text{H}$  bond length of 1.11 Å.

The intensity of the  $\text{C}\alpha$  peak reflects the dephasing of the  $\text{H}\alpha$  magnetization by the  $^{13}\text{C}\alpha$  spin. Since we detect only naturally occurring  $^{13}\text{C}\alpha$  spins, the  $\text{H}\alpha$  spins adjacent to a  $^{12}\text{C}\alpha$  nucleus are not observed in the spectra. In other words, all observed  $\text{H}\alpha$  spins are subject to the large one-bond  $^{13}\text{C}\alpha$ - $^1\text{H}\alpha$  dipolar interaction ( $\delta_{\text{CH}} = 22.7$  kHz) and their magnetization dephases

significantly. Simulations indicate that the magnetization evolves under an effective dipolar coupling of  $\delta_{\text{eff,CH}} = 48 \pm 5.0$  kHz, which is equivalent to  $\delta_{\text{CH}} = 21 \pm 2.2$  kHz, if the theoretical FSLG scaling factor of 0.577 is assumed. Near  $t_f = 16 \mu\text{s}$ , the powder-averaged magnetization of the  $\text{H}\alpha$  spin directly bonded to a  $^{13}\text{C}\alpha$  spin has its first zero-crossing, and its second zero-crossing occurs near  $t_f = 40 \mu\text{s}$ . These are suitable filter times for the MELODI-HETCOR experiment.

In contrast to the  $\text{C}\alpha$ – $\text{H}\alpha$  spin pair, the intensity of the two-bond  $^{13}\text{CO}$ – $^1\text{H}\alpha$  spin pair shows little C–H dipolar dephasing. The experimental intensity distribution can be simulated (Fig. 2) using an effective coupling of  $\delta_{\text{eff,CH}} = 5.0 \pm 1.0$  kHz. Using Eq. [1], this yields a C–H coupling of  $\delta_{\text{CH}} = 2.2 \pm 0.43$  kHz, which is in satisfactory agreement with the 2.4-kHz coupling calculated from the two-bond  $^{13}\text{CO}$ – $^1\text{H}\alpha$  distance of 2.14 Å.

The fit curves in Fig. 2 were obtained using REDOR powder simulations. The agreement is semiquantitative. The observed

deviations, for example, near the center of the rotation period for the one-bond coupling, may be due to orientation-dependent  $^1\text{H}$ – $^{13}\text{C}$  cross-polarization efficiencies or result from partial orientation of crystallites in the rotor. For the MELODI-HETCOR experiment, these deviations are insignificant: only the zero-crossings and the difference between the one- and two-bond dephasing curves are of interest.

**MELODI-HETCOR spectra.** Figure 3a displays the 2D MELODI-HETCOR spectrum of a mixture of unlabeled valine and alanine. The spectrum was acquired at a spinning speed of 7576 Hz with 700  $\mu\text{s}$  of LG-CP and a filter time  $t_f = 34 \mu\text{s}$ . This filter time was found to produce the best suppression of the one-bond peaks. The corresponding regular HETCOR spectrum is shown for reference in Fig. 3b. The signals of the directly bonded CH and  $\text{CH}_2$  protons, most notably the  $\text{C}\alpha$ – $\text{H}\alpha$  peaks of Val ( $\text{C}\alpha$ : 63.3 ppm) and Ala ( $\text{C}\alpha$ : 52.6 ppm), are cleanly suppressed in the

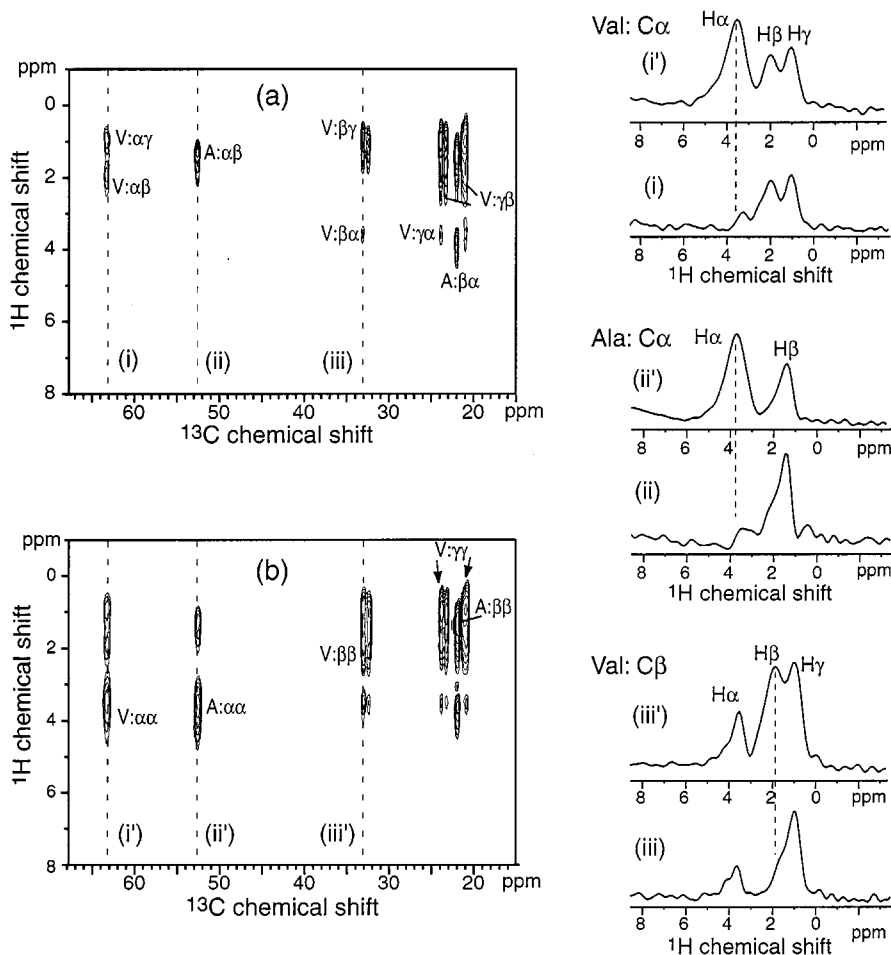


**FIG. 3.** 2D HETCOR spectra of a mixture of unlabeled alanine and valine. (a)  $^1\text{H}$ – $^{13}\text{C}$  MELODI-HETCOR spectrum, acquired with a filter time  $t_f = 34 \mu\text{s}$ . (b) Regular  $^1\text{H}$ – $^{13}\text{C}$  HETCOR spectrum for comparison. Resonance assignment is indicated by two Greek symbols that denote, sequentially, the  $^{13}\text{C}$  and  $^1\text{H}$  identities. Three cross sections parallel to the  $^1\text{H}$  dimension, corresponding to the Val  $\text{C}\alpha$  (i), Ala  $\text{C}\alpha$  (ii), and Val  $\text{C}\beta$  (iii) chemical shifts, are displayed for each 2D spectrum. Contour levels range from 15 to 100% of the maximum intensity of each 2D spectrum. The dwell time of the  $^1\text{H}$  dimension was 88  $\mu\text{s}$ . One hundred  $t_f$  points were collected, corresponding to a maximum evolution time of 8.8 ms.  $^1\text{H}$  chemical shifts were referenced to the Ala  $\text{CH}_3$  peak, which is set to 1.39 ppm according to the standard solution NMR value (30).  $^{13}\text{C}$  chemical shifts were referenced to external glycine  $^{13}\text{CO}$  at 176 ppm.

MELODI-HETCOR spectrum. The  $^1\text{H}$  resonances in the Val C $\beta$  cross section (32.8 ppm) show apparently reduced linewidths, since the signal of the directly bonded H $\beta$ 's that overlap with the H $\gamma$ 's is suppressed. This demonstrates the resolution enhancement achieved by the one-bond  $^1\text{H}$ - $^{13}\text{C}$  dipolar filter. Various  $^1\text{H}$  cross sections are displayed in Fig. 3 to illustrate the suppression of the directly bonded C-H cross peaks. Note that the methyl proton signals of Val and Ala are only partially attenuated by the dipolar filtration, since their C-H couplings are reduced by a factor of 3 as a result of the methyl-group rotational jumps.

The MELODI-HETCOR experiment is particularly useful if the normal HETCOR spectrum is crowded and one-bond correlation peaks overlap with those of medium- and long-distance correlation. It is directly complementary to HETCOR experiments with short dipolar transfer (17) or with *J*-coupling-based transfer (18, 19), which exclusively give signals of directly bonded protons.

The two-bond cross-peak intensities such as C $\alpha$ -H $\beta$  in the filtered and unfiltered HETCOR spectra are expected to be similar. In both cases, the magnetization of the H $\beta$  proton is not fully transferred to the protonated C $\alpha$  carbon of interest. In the MELODI-HETCOR experiment, the H $\beta$  magnetization (100%) is distributed over both the  $^{13}\text{C}\alpha$  spin (33% at equilibrium if the  $\beta$  segment is also a C-H group) and its directly bonded H $\alpha$  (33% at equilibrium). This reduces the C $\alpha$ -H $\beta$  signal intensity compared to the case when  $^1\text{H}\alpha$  is absent; for example, if the H $\alpha$  were replaced with a deuteron, the equilibrium magnetization of C $\alpha$  would be 50%. In the unfiltered HETCOR experiment, half of the  $^{13}\text{C}\alpha$  magnetization originates from H $\beta$  (33% at equilibrium) and half from H $\alpha$  (33% at equilibrium). Note that the transfer from the two-bond H $\beta$  to the directly bonded H $\alpha$  does not produce an undesirable signal component at the H $\alpha$  chemical shift in the MELODI-HETCOR spectrum.

It may be interesting to note that the dipolar filtering approach described here shares a similarity with proton-detected local field (20-23) experiments, since  $^1\text{H}$  rather than  $^{13}\text{C}$  magnetization is dephased. Dephasing of the  $^{13}\text{C}$  magnetization in the separated-local-field (24, 25) fashion would have a different and less useful effect, since it would remove the signals of all protonated carbons from the HETCOR spectrum, much like dipolar dephasing of  $^{13}\text{C}$  magnetization by gated decoupling (26).

It should be noted that the current one-bond suppression scheme is mostly not applicable to uniformly  $^{13}\text{C}$ -labeled molecules, because the magnetization of all protons other than N-H, O-H, and S-H protons would be dephased by the abundant  $^{13}\text{C}$  spins. However, selective and extensive  $^{13}\text{C}$  labeling schemes such as TEASE (27, 28) produce relatively isolated  $^{13}\text{C}$  spins and thus permit the application of the MELODI-HETCOR experiment to proteins.

## CONCLUSION

The one-bond proton-dipolar-filtered MELODI-HETCOR experiment is a promising and robust approach for simplifying

$^1\text{H}$ - $^{13}\text{C}$  HETCOR spectra and for enabling more extensive resonance assignment and chemical structure identification. The signals of directly bonded protons are suppressed without significant intensity loss of the long-range correlation peaks. The dephasing of the intensity of a given peak traces out a  $^1\text{H}$ - $^{13}\text{C}$  REDOR curve, and the experimental data show semiquantitative agreement with the simulations. The MELODI-HETCOR approach is promising for structural characterizations of complex organic solids and for extending the limit of resonance assignment of selectively  $^{13}\text{C}$ -labeled solid proteins. Further developments, such as broadening the one-bond filter condition and suppressing both one- and two-bond proton signals, are in progress.

## EXPERIMENTAL

**Materials.** The amino acids valine and alanine with  $^{13}\text{C}$  in natural abundance were obtained from Sigma and used without further purification; 53.2 mg of an equimolar mixture of alanine and valine was packed into the center of a 4-mm MAS rotor. Alanine- $d_6$  used for the filter time dependence study was prepared by dissolving 95% L-alanine- $d_3$  (C/D/N Isotopes, Inc., Vaudreuil, Canada) and 5% unlabeled L-alanine in  $^2\text{H}_2\text{O}$  for several hours and subsequent drying. The methyl-protonated L-alanine was added to reduce the recycle delay between experiments, by virtue of the fast methyl-proton  $T_1$  relaxation and spin diffusion to H $\alpha$ . A 60.2-mg sample of the mixture was packed in a 4-mm MAS rotor.

**NMR experiments.** All NMR experiments were carried out on a Bruker DSX-400 spectrometer (Karlsruhe, Germany) operating at a resonance frequency of 100.714 MHz for  $^{13}\text{C}$  and 400.497 MHz for  $^1\text{H}$  at room temperature ( $T = 293 \pm 1$  K). A double-resonance MAS probe equipped with a 4-mm spinning module was used. Frequency switching in the FSLG sequence was accomplished using a linear phase ramp (29). The phase ramp consists of a train of phase values incremented at  $10^\circ$  steps. A basic unit in the phase file consists of phase angles of  $0^\circ$ - $210^\circ$  and  $30^\circ$ - $180^\circ$ . The duration of each basic unit was synchronized with two  $360^\circ$  pulses around the FSLG effective field, which is tilted at the magic angle with respect to the magnetic field direction. The strength of the effective field was 90.9 kHz, which corresponded to a 11- $\mu\text{s}$   $360^\circ$  pulse. Lee-Goldburg cross polarization (17) was applied to suppress  $^1\text{H}$ - $^1\text{H}$  spin diffusion during the polarization transfer. A contact time of 700  $\mu\text{s}$  and a  $^1\text{H}$  spin lock field strength of 44.7 kHz were used. The  $^1\text{H}$  decoupling field during the acquisition period was 74.2 kHz. The  $^1\text{H}$   $90^\circ$  and  $35^\circ$  pulse lengths were 3.37 and 1.32  $\mu\text{s}$ , respectively. The MAS spinning speed was  $7576 \pm 2$  Hz, regulated by a Bruker spinning speed controller.

The filter time dependence experiment was carried out by incrementing the delay  $t_f$  from 4.16 to 112.5  $\mu\text{s}$  with a step of 3.875  $\mu\text{s}$ ; 32 time points were measured. Note that  $t_f$  includes half the pulse length of the 8- $\mu\text{s}$   $^{13}\text{C}$   $180^\circ$  pulse.

The C–H dipolar-modulated  $^1\text{H}$  dephasing curves as a function of the filter time were simulated using a Fortran program described earlier (16). The simulations were carried out for one rotation period, with the effective C–H dipolar coupling as the only adjustable parameter. Powder averaging was performed in  $3^\circ$  increments for all three Euler angles. Other input parameters were the spinning speed and the number of time domain points. Simulations were performed on a Macintosh G4 computer and analyzed using the MATLAB software.

### ACKNOWLEDGMENTS

M.H. gratefully acknowledges the Arnold and Mabel Beckman Foundation for a Young Investigator Award and National Science Foundation for a POWRE award (MCB-9870373). K.S.-R. thanks the Alfred P. Sloan Foundation for a Sloan Fellowship. The authors thank W. Hu for the preparation of the alanine sample.

### REFERENCES

1. P. Caravatti, L. Braunschweiler, and R. R. Ernst, HETCOR spectroscopy in rotating solids, *Chem. Phys. Lett.* **100**, 305–310 (1983).
2. C. W. B. Lee and R. G. Griffin, Two-dimensional  $^1\text{H}/^{13}\text{C}$  heteronuclear chemical shift correlation spectroscopy of lipid bilayers, *Biophys. J.* **55**, 355–358 (1989).
3. B. J. vanRossum, H. Forster, and H. J. M. deGroot, High-field and high-speed CP-MAS  $^{13}\text{C}$  NMR heteronuclear dipolar correlation spectroscopy of solids with frequency-switched Lee–Goldburg homonuclear decoupling, *J. Magn. Reson.* **124**, 516–519 (1997).
4. K. W. Zilm and G. G. Webb,  $^{13}\text{C}$  proton shift correlation spectroscopy of a whole coal, *Fuel* **65**, 721–724 (1986).
5. M. A. Wilson, J. V. Hanna, K. B. Anderson, and R. E. Botto,  $^1\text{H}$  CRAMPS NMR derived hydrogen distributions in various coal macerals, *Org. Geochem.* **20**, 985–999 (1993).
6. J. Mao, B. Xing, and K. Schmidt-Rohr, New structural information on a humic acid from two-dimensional  $^1\text{H}$ – $^{13}\text{C}$  correlation solid-state nuclear magnetic resonance, *Environ. Sci. Technol.*, in press, (2000).
7. A. Bielecki, D. P. Burum, D. M. Rice, and F. E. Karasz, Solid-state two-dimensional  $^{13}\text{C}$ – $^1\text{H}$  correlation (HETCOR) NMR spectrum of amorphous poly(2,6-dimethyl-*p*-phenylene oxide) (PPO), *Macromolecules* **24**, 4820–4822 (1991).
8. K. Saalwachter, R. Graf, D. E. Demco, and H. W. Spiess, Heteronuclear double-quantum MAS NMR spectroscopy in dipolar solids, *J. Magn. Reson.* **139**, 287–301 (1999).
9. A. Bielecki, A. C. Kolbert, H. J. M. de Groot, R. G. Griffin, and M. H. Levitt, Frequency-switched Lee–Goldburg sequences in solids, *Adv. Magn. Reson.* **14**, 111–124 (1990).
10. A. Bielecki, A. C. Kolbert, and M. H. Levitt, Frequency-switched pulse sequences: Homonuclear decoupling and dilute spin NMR in solids, *Chem. Phys. Lett.* **155**, 341–346 (1989).
11. U. Haebleren, “High Resolution NMR in Solids: Selective Averaging,” Academic Press, San Diego (1976).
12. D. P. Burum, M. Linder, and R. R. Ernst, Low-power multiple line narrowing in solid-state NMR, *J. Magn. Reson.* **44**, 173–188 (1981).
13. P. Mansfield, MREV8, *J. Phys. Chem.* **4**, 1444 (1971).
14. S. R. Hartmann and E. L. Hahn, Nuclear double resonance in the rotating frame, *Phys. Rev.* **128**, 2042–2053 (1962).
15. T. Gullion and J. Schaefer, Detection of weak heteronuclear dipolar coupling by rotational-echo double-resonance nuclear magnetic resonance, in “Advances in Magnetic Resonance” (W. S. Warren, Ed.), pp. 57–83, Academic Press, San Diego (1989).
16. M. Hong, J. D. Gross, C. M. Rienstra, R. G. Griffin, K. K. Kumashiro, and K. Schmidt-Rohr, Coupling amplification in 2D MAS NMR and its application to torsion angle determination in peptides, *J. Magn. Reson.* **129**, 85–92 (1997).
17. B. J. vanRossum, C. P. deGroot, V. Ladizhansky, S. Vega, and H. J. M. deGroot, A method for measuring heteronuclear ( $^1\text{H}$ – $^{13}\text{C}$ ) distances in high speed MAS NMR, *J. Am. Chem. Soc.* **122**, 3465–3472 (2000).
18. A. Lesage, D. Sakellariou, S. Steuernagel, and L. Emsley, Carbon–proton chemical shift correlation in solid-state NMR by through-bond multiple-quantum spectroscopy, *J. Am. Chem. Soc.* **120**, 13194–13201 (1998).
19. M. Baldus, R. J. Iulucci, and B. H. Meier, Probing through-bond connectivities and through-space distances in solids by magic-angle-spinning NMR, *J. Am. Chem. Soc.* **119**, 1121–1124 (1997).
20. K. Schmidt-Rohr, D. Nanz, L. Emsley, and A. Pines, NMR measurement of resolved heteronuclear dipole couplings in liquid crystals and lipids, *J. Phys. Chem.* **98**, 6668–6670 (1994).
21. M. Hong, K. Schmidt-Rohr, and A. Pines, Measurement of signs and magnitudes of C–H dipolar couplings in lecithin, *J. Am. Chem. Soc.* **117**, 3310–3311 (1995).
22. M. Hong and K. Schmidt-Rohr, DISTINCT NMR for sign determination of C–H dipolar couplings, *J. Magn. Reson. B* **109**, 284–290 (1995).
23. D. P. Weitekamp, J. R. Garbow, and A. Pines, Determination of dipole coupling constants using heteronuclear multiple quantum NMR, *J. Chem. Phys.* **77**, 2870–2883 (1982).
24. R. K. Hester, J. L. Ackermann, B. L. Neff, and J. S. Waugh, Separated-local-field spectra in NMR, *Phys. Rev. Lett.* **36**, 1081 (1976).
25. J. S. Waugh, Uncoupled local-field spectra in NMR: Determination of atomic positions, *Proc. Natl. Acad. Sci. USA* **73**, 1394 (1976).
26. S. J. Opella and M. H. Frey, Selection of non-protonated carbon resonances in solid-state nuclear magnetic resonance, *J. Am. Chem. Soc.* **101**, 5854 (1979).
27. M. Hong, Determination of multiple phi torsion angles in solid proteins by selective and extensive  $^{13}\text{C}$  labeling and two-dimensional solid-state NMR, *J. Magn. Reson.* **139**, 389–401 (1999).
28. M. Hong and K. Jakes, Selective and extensive  $^{13}\text{C}$  labeling of a membrane protein for solid-state NMR investigation, *J. Biomol. NMR* **14**, 71–74 (1999).
29. E. Vinogradov, P. K. Madhu, and S. Vega, High-resolution proton solid-state NMR spectroscopy by phase-modulated Lee–Goldburg experiment, *Chem. Phys. Lett.* **314**, 443–450 (1999).
30. J. N. S. Evans, “Biomolecular NMR Spectroscopy,” Oxford Univ. Press, Oxford (1995).